Cellulose (2024) 31:4461–4475
https://doi.org/10.1007/s10570-024-05899-5

ORIGINAL RESEARCH

Transparent, mechanically robust, low-temperature-tolerant, and stretchable ionogels enhanced by konjac glucomannan toward wireless strain sensors

Zhifan Ye · Min Yang · Yijia Zheng · Qihan Jia · Haibo Wang · Junjie Xiong · Shuang Wang

Received: 23 May 2023 / Accepted: 5 April 2024 / Published online: 15 April 2024

Abstract Electronic skins (*E*-skins) can detect human health and movement, and have potential in the fields of human–machine interactions and artificial intelligence. However, traditional hydrogel-based *E*-skins suffer from poor mechanical strength, low conductivity, and instability due to water evaporation. Herein, a semi-interpenetrating network developed by polysaccharide biomass konjac glucomannan (KGM) was introduced into a covalent-crosslinked network polyacrylamide-*co*- polyacrylic acid (PAM-*co*-PAA) to advance the above dissatisfaction of *E*-skins. This synthesized a transparent, tough, nonvolatile, and highly stretchable ionogel with an ionic liquid named 1-ethyl-3-methylimidazolium dicyamide (EMIM:DCA) as conductive media. This ionogel exhibited extraordinary mechanical strength (tensile strength of 2.77 MPa), outstanding mechanical durability (100 stretching cycles of 250%), and elongation (elongation at break of 997%). More importantly, the ionogel demonstrated remarkable anti-freezing performance (high flexibility at -20℃) and high conductivity (3.94 mS/cm) in the absence of water. Besides, after assembling KGM-enhanced ionogel, the sensor exhibited comprehensive strain sensing performance, which could effectively and accurately monitor human motion via Bluetooth transmission. This strategy paves the way for a viable new generation of multifunctional biomimetic supersensitive sensors, which are promising for applications such as intelligent devices, health detection, and biomedical monitoring in harsh conditions.

Zhifan Ye, Min Yang contributed equally to this work.

Z. Ye · Y. Zheng · Q. Jia · J. Xiong (✉)
Department of Pancreatic Surgery, West China Hospital, Sichuan University, Chengdu 610041, China
e-mail: junjiex2011@126.com

Z. Ye · Y. Zheng · H. Wang · S. Wang (✉)
College of Biomass Science and Engineering, Sichuan University, Chengdu 610065, People's Republic of China
e-mail: shuangshine7@scu.edu.cn

M. Yang
Department of Pediatric Surgery, West China Hospital, Sichuan University, Chengdu 610041, China

Graphical abstract

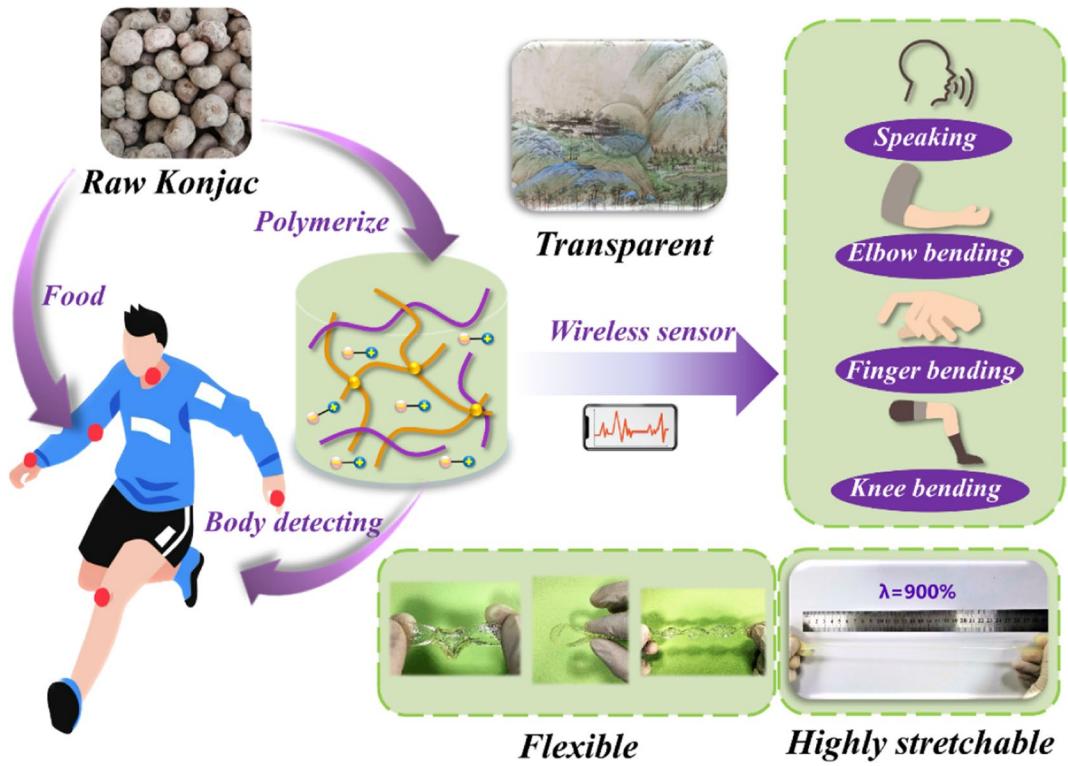

Keywords Konjac Glucomannan · Ionogels · Strain sensor · Biomass · Wearable device

Introduction

With the rise of flexible electronic devices, synthesizing biomass-based flexible tensile sensors with high sensitivity, high tensile strength, and stable performance has become significant for physical health and smart wearable devices (Chen et al. 2021; Wang et al. 2021; Zhou et al. 2022; Zhu et al. 2022). Traditional conductive materials, such as carbon nanotubes and graphene, do not have the capacity for stretchability, and their complex internal structures are difficult to achieve, which also limits the transparency of the material (Hou et al. 2019; Huang et al. 2023; Liao et al. 2017; Lipomi et al. 2011; Pang et al. 2018). Conversely, conductive gel has already become a novel material for wearable sensors, with the advantages of easy manufacturing, excellent flexibility, and high biocompatibility.

At present, the conductive gel material substrate is mainly hydrogel, widely applied in health care, biosensors, and human–machine interactions (Chen et al. 2022). Although its fantastic flexibility, biocompatibility, and conductivity are shown in recent research, under the influence of water evaporation in the hydrogel, its sensitivity, mechanical robustness, stability, and conductivity would dramatically decrease, limiting its extensive use as wearable sensors. Therefore, it is significant to manufacture a wearable sensor with high conductivity, non-volatile properties, high stretchability, and high stability (Xue et al. 2023).

Ionogels are formed by the polymer network swelling process in the ionic liquid, which has heat stability, high ionic conductivity, electrochemical stability, and non-volatile properties (Huang et al. 2023; Kim et al. 2023; Li et al. 2023; Wang et al. 2022a, b, c; Jiang et al. 2021). Chemical gelling is mainly used for preparation, and other conductive materials are also added to obtain better mechanical and electrochemical properties. Sun et al. (2021) synthesized a kind of

dual-network (DN) ionogel with excellent mechanical properties, high transparency, wide operating temperature range, and strong adhesion prepared by photopolymerization method. The gel synthesis was based on an agar network and formed an interpenetrating network by introducing polyhydroxyethyl acrylate into an ionic solution. The excellent mechanical properties and sensing properties of this ionogel enabled it to be used as a flexible strain sensor to detect human joint movement and pulse. Xiang et al. (2022) prepared another kind of ionogel material (IL-PILs-IG) by copolymerizing 1-vinyl-3-butylimidazole tetrafluoroboric acid ([VBIm]) and 1-dodecyl-3-tetrafluoroboric acid ($[C_{12}VIm][BF_4]$) in non-polymeric ionic liquid 1-butyl-3-methylimidazole ([BMIm][fluoborate]) in the one-pot method with favorable tensile properties, high transparency (91%), high thermal stability (> 300 °C), and remarkable recovering property. Therefore, the important role of ion-hydrophobic "microdomains" composed of $[C_{12}VIm]^+$ long alkyl chains in improving mechanical properties was confirmed. In this regard, ionic liquid (1-ethyl-3-methyl imidazole dihydro amine salt, EMIM:DCA) was applied as a solvent to prepare a biomass-based composite ionogel with high conductivity, non-volatile properties, and high mechanical properties.

Biodegradable biomass materials, such as collagen, cellulose, and chitosan, are receiving increasing attention and are widely used in biomedicine, adsorption and catalysis, energy storage, and flexible electronics (Hajiali et al. 2022; Rezaei et al. 2021; Seabra et al. 2018; Strauss and Chmielewski 2016). Researchers have used many biopolymer materials to construct flexible strain sensors (Ahmed et al. 2016; Kalambate et al. 2020; Rezaei et al. 2021). Konjac glucomannan (KGM) is a water-soluble, neutral, natural heteropolysaccharide with high molecular weight and hydrophilic groups such as active primary hydroxy ($-CH_2OH$) and acetyl groups (Gao et al. 2022; Hu et al. 2019; Wu et al. 2020; Zhu 2018). KGM consists of β-D-mannose and β-D-glucose. The molar ratio of glucose to mannose is 1.6:1 and they are connected through β-1,4-glycosidic bonds. Moreover, acetyl groups attach to the saccharide units and distribute randomly along the molecule, with an occurrence of 1 per 19 sugar residues at the C (6) position. It is popular in developing biomedical materials and functional food formulations (Cao et al. 2022; Zhang et al. 2023; Wu et al. 2022a, b). Introducing KGM forms a semi-interpenetrating network in the original PAM-*co*-PAA network, and the functional groups enabled it to enhance the mechanical properties of the ionogel. Xu et al. (2022) adopted polyvinylidene fluoride-*co*-hexafluoropropylene (PVDF-HFP) as the linear non-cross-linked network in the ionogel, and strain strength increased with the addition of PVDF-HFP (3.67 to 8.76 MPa) due to an increase in cross-linking points. Wang et al. (2021) involved 2,2,6,6-tetramethylpiperidinyl-1-oxyl-oxidized cellulose nanofibril (TEMPO-CNF) in the hydrogel with covalently cross-linked polyacrylamide and formed a DN structure. Its elongation at break was 1100%, and its tensile strength was 710 kPa. However, there are few studies on applying KGM to flexible ionogel-based sensors. Hence, it was considered that KGM, as a kind of biomass-based polymer polysaccharide material, has the potential to enhance the toughness, stretchability, resilience and flexibility of ionogels. There are few studies on the application of KGM in ionogel-based flexible sensors.

Herein, we introduced KGM polysaccharide biomass into the ionic liquid to prepare a transparent, mechanically robust, and anti-freezing ionogel. First, KGM was dissolved in EMIM:DCA to obtain the KGM/ionic liquid mixture, and then acrylamide (AM) and acrylic acid (AA) were dispersed in the above mixture. After that, the mixture was exposed to ultraviolet (UV) light to form a semi-interpenetrating network-enhanced KGM/PAM-*co*-PAA ionogel. Simultaneously, EMIM:DCA provided high conductivity, non-volatile, and anti-freezing properties due to its various beneficial properties. Importantly, KGM is a biomass-based and environmentally friendly material. Therefore, after mixing and gelling in an EMIM:DCA solution, an ionogel-based *E*-skin was proposed, which had several attributes of being mechanically strong, highly conductive, biocompatible, and highly self-recovering. Notably, this enhanced hydrogen bond effect was proven to endow ionogels with tensile strength, self-recovering properties, and elongation at break. Furthermore, we demonstrated the potential value of the assembled ionogel sensors in different application scenarios (finger bending, neck bending, running, and jumping). It confirmed that our study will help designers and manufacturers create multifunctional wearables with various use cases.

Experiment section

Materials

Konjac Glucomannan (KGM, viscosity ≥ 15,000 mpa.s) was supplied by Shanghai Yuanye Bio-Technology Co., Ltd. (Shanghai China). 2-hydroxy-4'-(2-Hydroxyethoxy)-2-methylpropiophenone (Irgacure 2959) and *N, N'*-Methylene-bis-acrylamide (MBAA Catalyst) was obtained from Shanghai Titan Science Co., Ltd. (Shanghai China). Acrylamide (AM) and acrylic acid (AA) were supplied from Aladdin Reagent Inc. (Shanghai, China). 1-ethyl-3-methylimidazolium dicyamide (EMIM:DCA, Ionic liquid) was obtained from Monils (Nanjing) Technology Co., Ltd.

Synthesis of PAM-co-PAA ionogel

Firstly, dewatering treatment of raw materials was given to AM and MBAA in a vacuum environment at 120 °C for 2 h. Secondly, 8.0 g EMIM:DCA, 2.0 g AM, 2.0 g AA, 12.0 mg MBAA were mixed and stirred at room temperature for 10 min to get a uniform mixture named IG (KGM content: 0 wt%). Then the photoinitiator was added to the IG solution. After that, the mixture was stirred for 10 min, and then placed in a vacuum to remove the bubbles for 20 min. Finally, it was gelled under UV light for 15 min and the ionogel sample was obtained which was named IKG-I_0.

Preparation of Konjac Glucomannan ionogel (Labeled IKG-I_x ionogel)

The detailed process of synthesizing IKG-I_x is shown in Scheme 1. Varied mass of IG solution (12.0 g, 9.3 g, 6.7 g, 4.0 g) was mixed with varied mass of IKG (KGM content: 6 wt%) solution (0 g, 2.7 g, 5.3 g, 8.0 g), making the total mass of the mixture 12.0 g with different KGM contents (0 wt%, 2.0 wt%, 4.0 wt%, and 6.0 wt%), which were denoted as IKG_0, IKG_2, IKG_4, and IKG_6. Then the photoinitiator was added to the IKG solutions. After that, the mixed solution was magnetically stirred for 20 min and then disposed of in a vacuum environment for 20 min with a preservative film covering their bottlenecks to prevent the evaporation of AA. After pouring the solution into PTFE moulds for molding and using UV light to initiate free radical polymerization, ionogel samples were obtained and named IKG-I_0, IKG-I_2, IKG-I_4, and IKG-I_6, respectively.

Characterization

Fourier transform infrared spectroscopy (FT-IR) was carried out with a Nicolet 560 FTIR spectrometer (Nicolet, USA) in the range from 4000 cm^{-1} to 650 cm^{-1} under a resolution of 4 cm^{-1} at ambient temperature with a total accumulation of 16 scans to evaluate the chemical structures and elemental components of konjac glucomannan and IKG-I_x. Moreover, the ultraviolet–visible (UV–vis) spectra of IKG-I_x were tested by the Analytik-Jena spectrophotometer S600 (Germany), ranging from 300 cm^{-1} to 800 cm^{-1}.

Scanning electron microscopy (JEOL TSM-7500F, Japan) was carried out to investigate the morphologies of IKG-I_4 and IG. IKG-I_4 and IG were quenched in nitrogen and lyophilized for 2 days. The samples above were then sputtered with gold to get conductivity.

The mechanical properties of different samples were tested by Instron 5967 universal tensile testing machine (Instron Electron Instrument Co. Ltd., USA). To ensure the experiments' reproducibility, tensile tests (cyclic test and single test) were performed on the three flat rectangular dumbbell-shaped samples with 30 mm (length) × 2 mm (thickness) × 4 mm (width), at room temperature, and the measurement rate was 50 mm min^{-1}, respectively. The results were expressed as the average of three readings taken for each measurement.

The rheological properties were recorded on a rheometer (MCR 302, Germany) at 25 ℃ using a parallel plate with a diameter of 25 mm at 1 mm gap. The frequency-sweep test was performed from 0.1 to 100 rad s^{-1} at a fixed strain of 0.1%. The strain-sweep was assessed in the strain range of 0.01–100% at a fixed frequency of 10 Hz. Cyclic strain time scanning was measured at a constant frequency of 10 Hz, and time scanning of low strain 0.1% and high strain 100% was carried out alternately. Each test section lasted for 100 s, and a total of 10 test Sects. (5 cycles) were conducted. All of the testing was done at 25 ℃.

The electrochemical workstation (PARSTAT MC, USA) was used to test the electrochemical performance of IG and IKG-I_x. Besides, the conductivity of ionogel samples was calculated from Formula (1):

$$\sigma = L/(R \times S) \tag{1}$$

where σ, L, R, and S are the conductivity, thickness, resistance, and cross-sectional area (CSA) of the samples respectively. The experiments' reproducibility

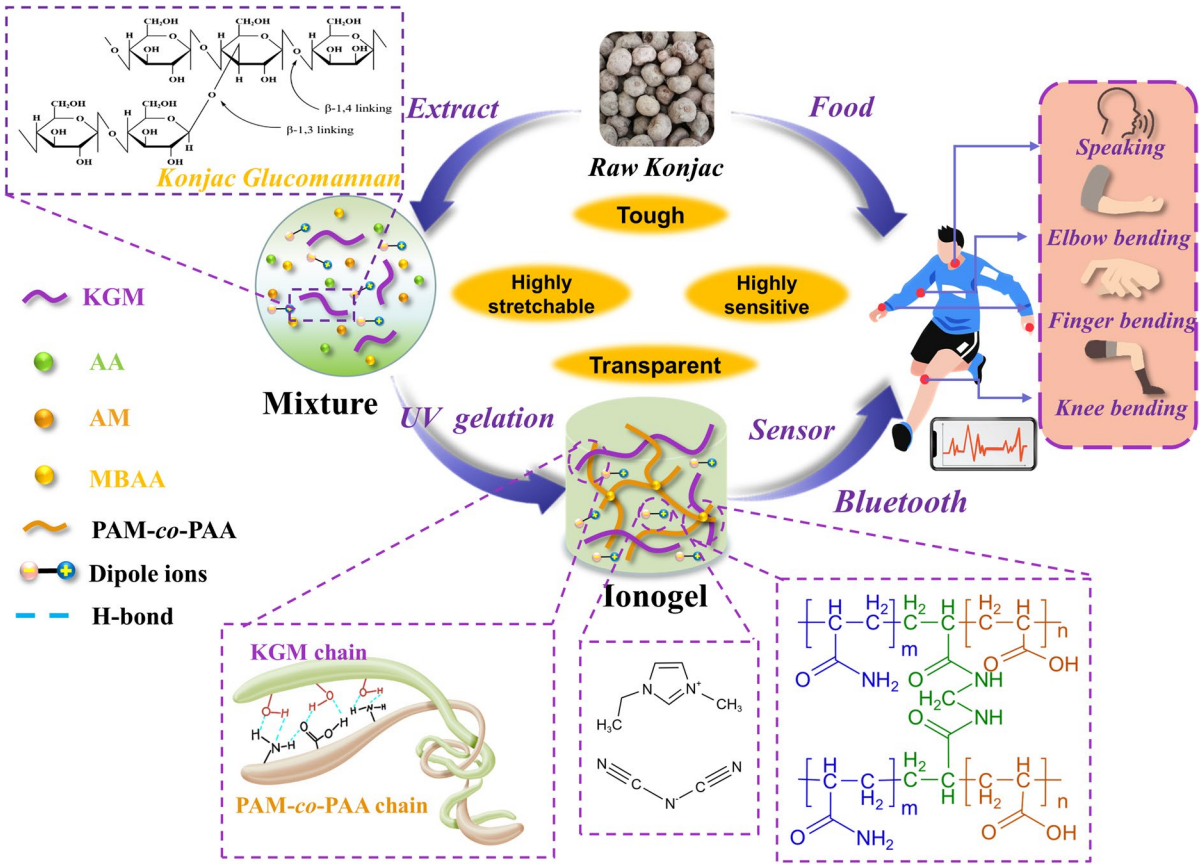

Scheme 1 Schematic of the preparation and application of IKG ionogels

was ensured by testing the electrochemical performance (conductivity and response time) with three flat rectangular specimens.

To measure the real-time relative resistance changes of duplicated samples, they were clamped by copper sheets on both sides as contact electrodes, and the PARSTAT MC, which had already been paired with a cellphone through a Bluetooth device, was connected to both ends of the sample by wires.

The thermal properties of IG and IKG-I_x were analyzed by a differential scanning calorimeter (DSC, 204F1, NETZSCH, Germany). Samples were implanted in an aluminum pan under a heating–cooling cycle in the range of -50 ℃ to 100 ℃ at 10 ℃ per minute.

In order to study the stability of ionogels in an ambient environment, weight losses of ionogels and hydrogels were carried out by the traditional gravimetric method in triplicate, and the average of three tests is used as the result.

Result and discussion

Synthesis and characterization

In this work, KGM biomass material was first dispersed in an EMIM:DCA solution to obtain a uniform mixture of KGM and ionic liquid. Thus, IKG-Ix ionogel was prepared by free radical copolymerizing AM and AA monomers in KGM-IG dispersion. At last, the PAM-*co*-PAA covalent cross-linked network bridged the KGM chains through physical entanglement interactions and hydrogen bonding (Wang et al. 2021; Wu et al. 2022a, b; Gao et al. 2023; Zhu et al. 2020). The snapshot in Fig. 1a shows the high transparency of IKG-I_4 when applied to a colorful picture beneath. As shown in Fig. 1b, the transmittance of IKG-I_0 reached 95%, ranging from 800 to 1000 nm. As the KGM content increased, the transmittance of IKG-I_2, IKG-I_4, and IKG-I_6 was 90%, 84%, and 75%,

respectively. The above results indicate that the KGM matrix had high miscibility and homogeneity with EMIM:DCA. In addition, IKG-I_4 showed excellent transparency (84%), greatly expanding the practical application range of IKG ionogels (Jiang et al. 2021).

Fourier-transform infrared spectroscopy (FT-IR) and UV–visible (UV–vis) spectra were recorded to study the chemical composition of IG and IKG-I_x. As shown in Fig. 1c, the peak at 1341 cm^{-1} corresponds to the stretching vibration of C-N belonging to PAM, while the peaks at 3431 and 1640 cm^{-1} are attributed to the N–H, O–H, and C=O bending vibrations of PAA and PAM. The peak at 1456 cm^{-1} is assigned to the bending vibration of -CH_2, and the stretching vibration of C=O can be related to 1722 and 1166 cm^{-1}, illustrating the -COOH group in PAA. Additionally, the peak at 3431 cm^{-1} is attributed to the -OH group, and a series of peaks from 1370 to 1454 cm^{-1} are the bending vibration of -CH_2 in -CH_2OH, indicating the existence of KGM. Moreover, under the influence of N on the imidazole ring, the asymmetric stretching vibrations of C-H were at 1460 and 1428 cm^{-1}, and the peaks at 3159 and 3105 cm^{-1} are the stretching vibrations of the two adjacent C-H on the imidazole ring of EMIM:DCA. The peak at 2203 cm^{-1} indicates C≡N of the negative ion in EMIM:DCA (Kabanda and Bahadur 2023). As a result, the PAM-*co*-PAA ionogel was successfully synthesized, and KGM biomass material was introduced in the covalently cross-linked networks to obtain a PAM-*co*-PAA/KGM DN ionogel.

Scanning electron microscopy (SEM) images of the freeze-dried IKG-I_0 surface in Fig. 1d–f exhibit an uneven structure with distributed large pores. On the

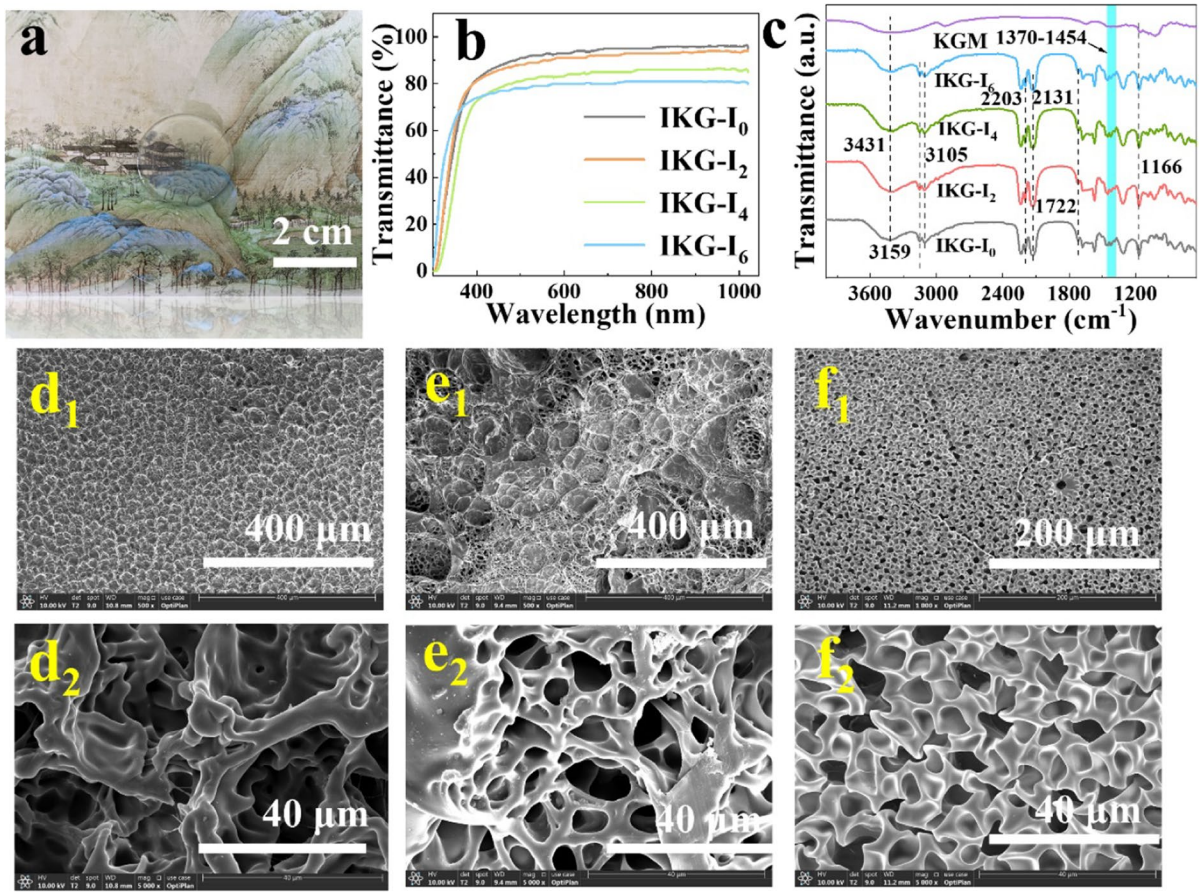

Fig. 1 **a**) Photograph demonstrating the transparency of IKG-I_4. (**b**) Transmittance curves of ionogels. (**c**) FT-IR spectra of KGM, IKG-I_0, IKG-I_2, IKG-I_4, IKG-I_6. SEM images of (**d**) IKG-I_0, (**e**) surface of IKG-I_4 and (**f**) fracture surface of IKG-I_4 at different magnifications

contrary, IKG ionogels showed a dense pore structure (Fig. 1e) on their surface. The aperture size was much smaller than IKG-I_0, showing a more robust honeycomb structure derived from hydrogen bonding between hydroxy groups of KGM chains and carboxyl/amidogen groups of PAM-*co*-PAA chains (Kim et al. 2020). This resulted in increased pore density and ensured the stability and stretchability of the IKG ionogel. Therefore, with its serried porous structure, IKG-I_4 could withstand high stress and elongation and recover rapidly from deformation.

Mechanical performances

Mechanical properties are one of the essential performances of flexible sensors. KGM, which introduced the semi-interpenetrating network into the IKG ionogels, endowed the IKG-I_x with excellent toughness, stretchability, resilience, and flexibility. Figure 2a shows that IKG-I_4 could resist 900% stretching of its initial length, enabling the ionogels to sustain all kinds of external stimuli without visible cracks. Ionogels with different KGM contents were tested by a universal tensile machine to investigate the tensile properties and durability of ionogels. IKG-I_0 showed poor tensile strength (0.35 MPa) and elongation at break (559%). As the KGM content increased to 1.0 wt%, tensile strength and elongation at break increased to 1.16 MPa and 973%, respectively. Moreover, the toughness increased from 1.13 to 4.73 MJ/m^3, and Young's modulus increased from 0.14 to 0.21 MPa.

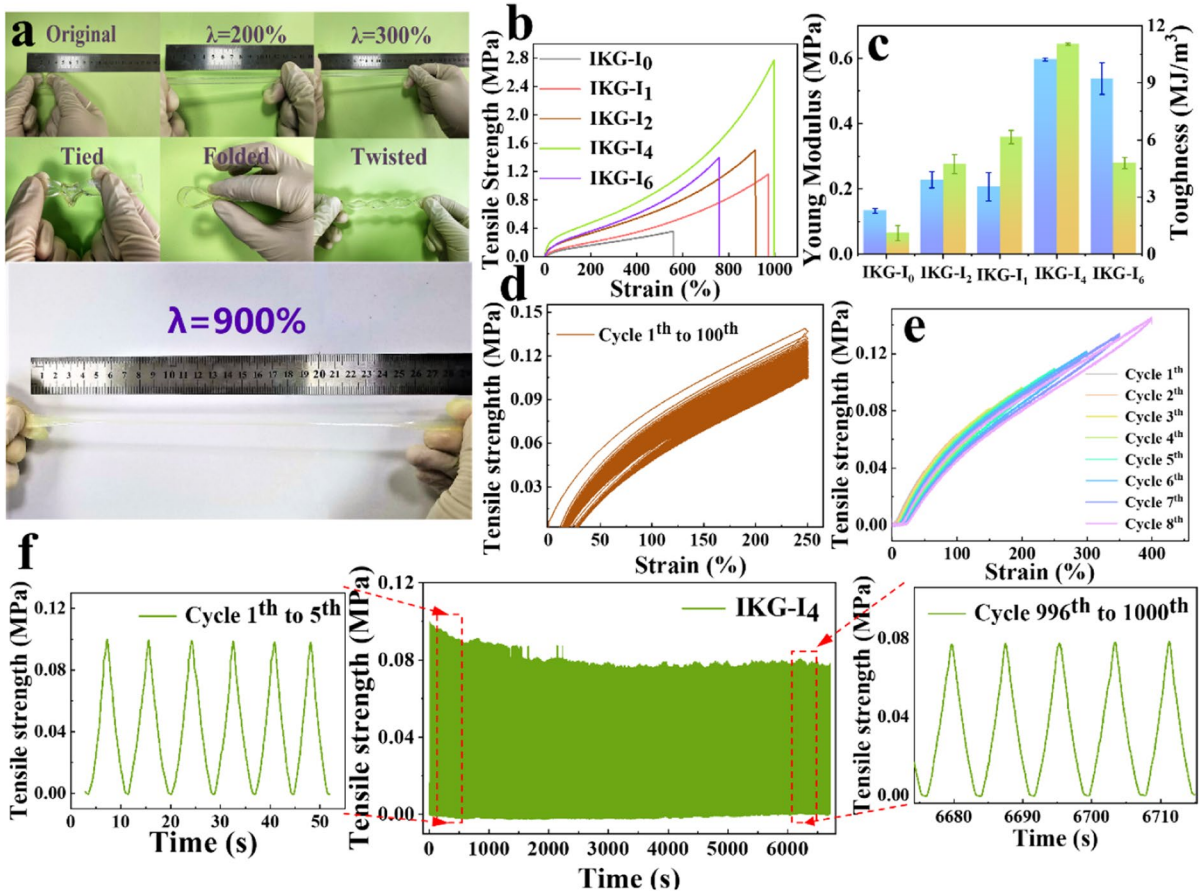

Fig. 2 Mechanical properties of ionogels (**a**) Snapshots of IKG-I_4 under external stimuli (stretch, tie, fold, twist). (**b**) Tensile stress–strain curves and (**c**) Toughness and Young's modulus of ionogels with different content of KGM. (**d**) Stress data of 100 cycles of the IKG-I_4 at 250%. (**e**) Tensile loading–unloading tests of the IKG-I_4 at different setting strains (50%, 100%, 150%, 200%, 250%, 300%, 350%, and 400%). (**f**) 1000 stretching cycles of stress-time curves

When the KGM content increased to 2.0 wt%, its tensile strength, toughness, and Young's modulus increased to 1.500 MPa, 6.15 MJ/m^3, and 0.28 MPa, respectively, but elongation at break decreased to 914%. IKG-I_4 showed superior mechanical properties; tensile strength became 2.77 MPa, the elongation at break reached 997% (in Fig. 2b), the toughness of IKG-I_4 reached 11.04 MJ/m^3, and Young's modulus was 0.60 MPa (in Fig. 2c). However, when KGM content was further increased to 6.0 wt%, tensile strength, elongation at break, toughness, and Young's modulus decreased to 1.392 MPa, 758%, 4.79 MJ/m^3, and 0.31 MPa, respectively, due to the synergistic effect of the DN density and defects (Xie et al. 2021). In this case, IKG-I_4 (tensile strength of 2.77 MPa and elongation at break of 997%) was the optimal choice for the following tests.

As shown in Fig. 2d, when the tensile test was at 250%, it could complete 100 strain cycles without breaking or cracking. This indicates that increasing the cycle number caused a change in the dissipated energy. Moreover, the loading–unloading tensile curves of IKG-I_4 displayed remarkable overlap after finishing the first cycle, and its self-recovery rate reached 77.6% after 1000 cycles (Fig. 2f), indicating its excellent anti-fatigue properties and durability. The hysteresis during the stretching cycles illustrates that the hydrogen bonds in IKG-I could break to dissipate energy. The slight decrease in maximum stress in successive cycles is attributed to the requirement of time to recover dynamic hydrogen bonds. Therefore, the tensile strength tended to decrease during stretching cycles (Zhou et al. 2023). A tensile stress–strain test was also carried out at eight different strains (50%, 100%, 150%, 200%, 250%, 300%, 350%, and 400%). As seen in Fig. 2e, the curves coincided, proving the stability of IKG-I_4. Therefore, the semi-interpenetrating network introduced by KGM improved the comprehensive mechanical properties and obtained favorable resilience. This allowed the IKG-I_x to build resilient, robust, and durable strain sensors.

Anti-freezing performance

Frost resistance plays an important role in broadening the applicable temperature range of flexible sensors. Differential scanning calorimetry (DSC) was carried out to measure the glass transition temperature (T_g) of IKG-I_4 and hydrogel in the range from -55 to 100℃ to further study the anti-freezing performance of ionogels. As observed in Fig. 3a and b, when the temperature decreased (-20℃), the flexibility and transparency of hydrogel decreased dramatically, but the IKG-I_4 maintained favorable flexibility and transparency. Still, the IKG-I_4 exhibited excellent transparency and could stand the twisting deformation and maintain flexibility. This illustrates that the IKG-I_4 could withstand -20℃ without a decrease in its flexibility. As shown in Fig. 3c, the weight loss of IKG-I_4 was 1.2 wt% after 20 days. However, the PAM-*co*-PAA hydrogel exhibited 60.0 wt% weight loss, indicating excellent stability of IKG-I_4 exposed to the ambient environment. Moreover, as seen in Fig. 3d, there was a prominent exothermic peak at 0 °C in the curve of the PAM-*co*-PAA hydrogel. On the contrary, the T_g was -43℃ for the ionogels owing to the extremely low freezing point of the EMIM:DCA. Therefore, in this work, the ionogel had favorable anti-freezing and water retention properties when exposed to air. This completely complies with the requirements of the wearable sensors used in extreme environments.

Rheological properties

First, ionogels with different KGM contents were tested by frequency scanning. Figure 4a shows the apparent frequency-dependent behaviors of the storage modulus (*G'*) and loss modulus (*G''*) in the range from 0.1 to 100 rad s^{-1}. Every sample maintained ideal elasticity. This was found by the phenomenon that the *G'* values of IKG-I_x were all greater than *G"* values in the whole frequency range. As the KGM content increased, the *G* curve had a higher value. However, when the KGM content exceeded 4.0 wt%, excessive cross-linking density and hydrogen bonding between PAM-*co*-PAA and KGM chains constrained the movement of the PAM-*co*-PAA network and the elastic properties of KGM chains. This led to an increase in the *G"* value and a decrease in the elastic nature of ionogels. Amplitude scanning was carried out (Fig. 4b) to investigate the effect of the KGM content on the mechanical properties. As the strain range was from 0.1% to 1.48%, G' and G" values maintained steady, indicating it was the linear viscoelastic region. When the strain was greater than 1.48%, *G'* and *G"* started to decrease. Furthermore, the increase

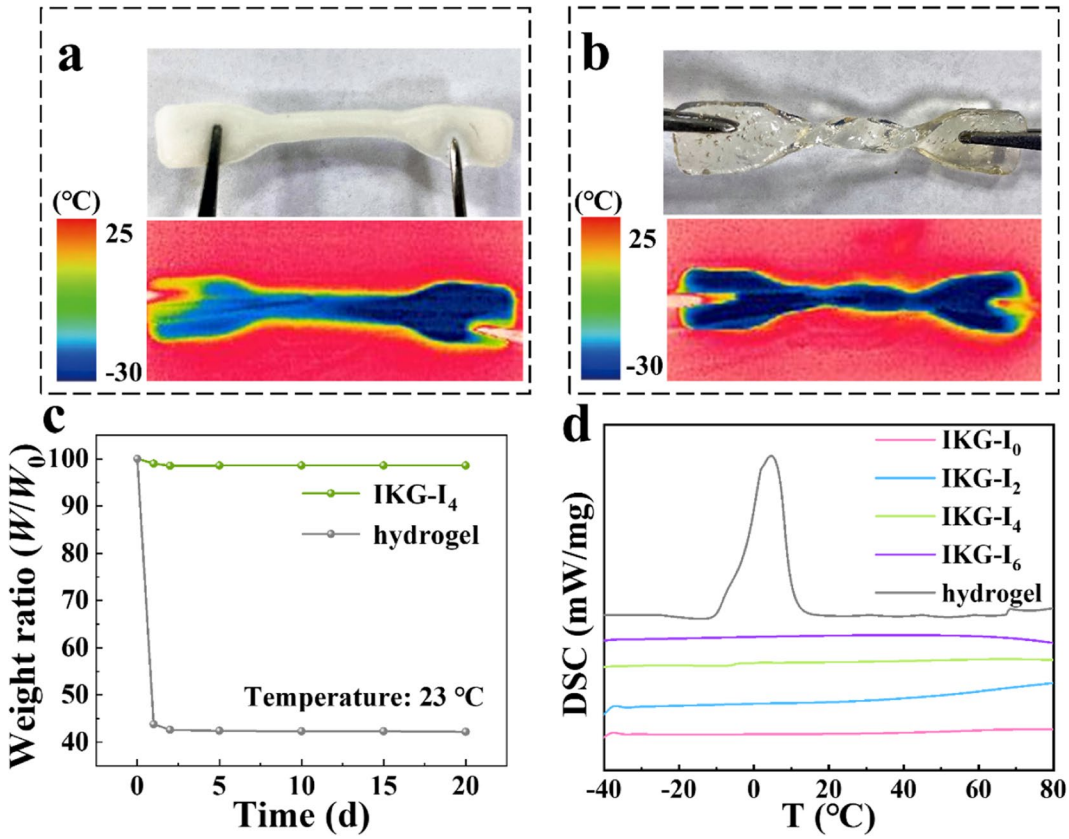

Fig. 3 Low temperature tolerance of (**b**) IKG-I_4 comparing with (**a**) PAM-*co*-PAA hydrogel. (**c**) Weight change of IKG-I_4 and PAM-*co*-PAA hydrogel at room temperature. (**d**) DSC curves of IKG-I_x and PAM-*co*-PAA hydrogel

in the KGM content generated an increase in the *G'* value in the range of 0 to 4.0 wt%, but the G' value gradually decreased when the KGM content exceeded 4.0 wt%. This was because KGM chains could improve the toughness of ionogels. On the contrary, the over-linked structure formed by the hydrogen bonding between KGM chains and the PAM-*co*-PAA network could lead to the over-rigidity of materials (Wang et al. 2022a, b, c), which reduces flexibility. Cyclic strain–time scanning was carried out (Fig. 4c and d) to further study the thixotropy influenced by the KGM content. It can be observed that both IKG-I_0 and IKG-I_4 performed typical elastic states at the strain range of 0.1% to 100%, and the recovery rate of IKG-I_4 in six cycles (85.47%) was higher than that of IKG-I_0 (84.87%). The phenomenon above proved that adding KGM improved the structural stability to a certain extent, and KGM chains increased the cross-linking density, which led to the high stiffness of IKG-I_4.

Electromechanical properties

The ionogels were installed as strain sensors to put them into use. So, they should be capable of transforming mechanical deformations into electrical signals through the change in resistance (ΔR) and possess excellent durable sensing ability. EMIM:DCA contained zwitterion, which could deliver electrons and give the ionogel conductivity. Besides, IKG-I_x was constituted by a cross-linked DN and EMIM:DCA. Under the electric field, the dipole ions of EMIM:DCA migrated toward different directions, giving the ionogel conductive properties (Wang, et al. 2022a, b, c). Additionally, the DN also gave IKG-I_x conductive pathways. When the sensor was deformed,

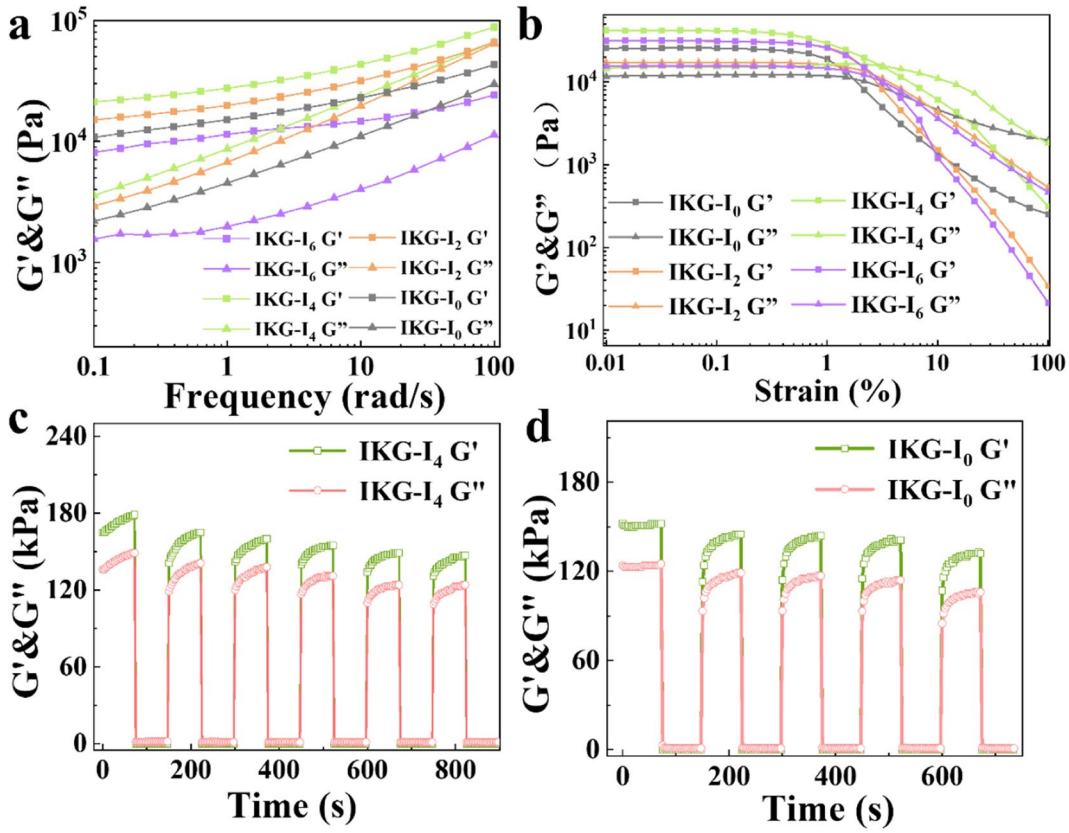

Fig. 4 The elastic modulus *G'* and loss modulus *G"* as a function of (**a**) frequency and (**b**) strain of ionogels with different content of KGM. (**c**) The cycle strain time sweep of IKG-I_4 and (**d**) IKG-I_0 under the action of low strain (0.1%) and high strain (100%)

it also narrowed the ion migration channels and caused a change in resistance (Scheme 2). Figure 5a shows that as the KGM content increased, the conductivity of the ionogel sensor declined slightly; the conductivity of IKG-I_0 reached 4.77 mS/cm. When the KGM content increased to 2.0 wt%, its conductivity decreased to 4.44 mS/cm. Ionogels with 4.0 wt% KGM still demonstrated excellent conductivity (3.94 mS/cm), and the conductivity of IKG-I_6 was 3.44 mS/cm. Moreover, as presented in Fig. 5b, the change in resistance demonstrated different variations under various stretching circumstances. In different frequencies (0.344, 0.156, and 0.125 Hz), the sensors were stretched at a fixed strain of 100%. It is shown

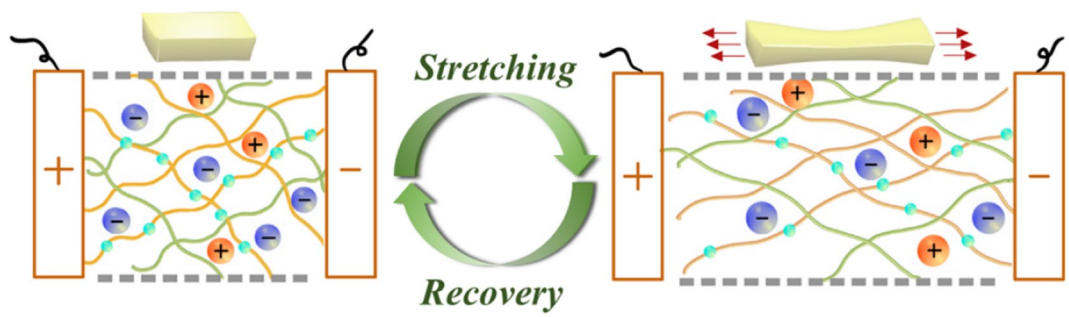

Scheme 2 Schematic demonstration of the conductive mechanism of IKG-I_4

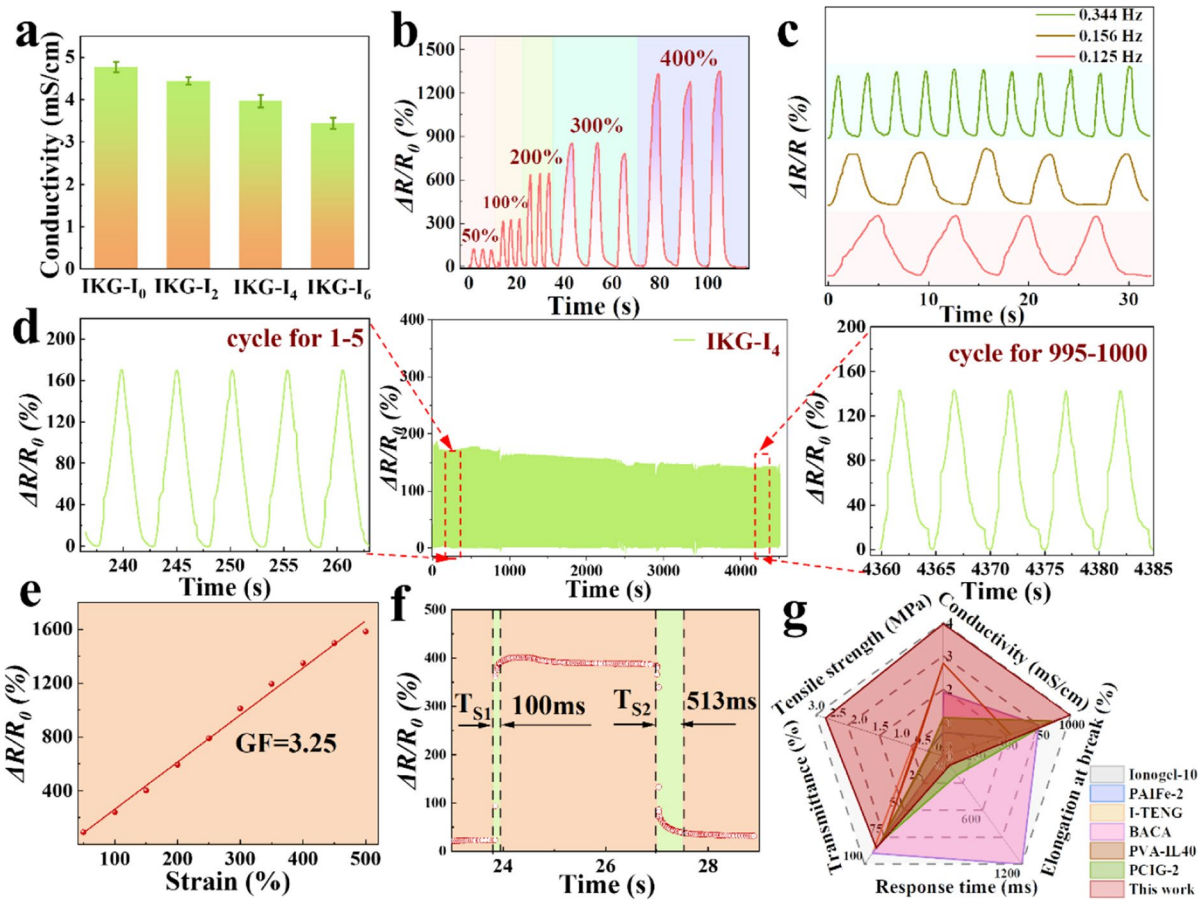

Fig. 5 **a** Conductivity of ionogels with different content of KGM. (**b**) The evolution of the $\Delta R/R_0$ signals under different strains (50%, 100%, 200%, 300%, and 400%). (**c**) Cyclic stretching-relaxing under different frequencies. (**d**) Relative resistance variation of the IKG-I_4 sensor under 100% strain for 1000 cycles. (**e**) The gauge factor of the IKG-I_4 as strain sensors. (**f**) Response time of IKG-I_4 during stretching-relax process. (**g**) Comparison of the IKG-I_4 and other ionogels in the literature in terms of conductivity, tensile strength, transmittance, response time and elongation at break

in Fig. 5c that the electric signal increased as the tensile strain of the sample augmented. Noticeably, the sensor showed superior durability and stability during the continuous stretching-release test at 100% tensile strain for 1000 cycles (84.6% self-recovery ratio). The curves in the tests above changed steadily during the cycle (Fig. 5d). The sensitivity of the installed sensor was evaluated by the gauge factor (GF) (Xiang et al. 2022), which is defined as the slope of the current-strain curve. $GF = \Delta(\Delta R/R_0)/\Delta\varepsilon$, where $R = R_t — R_0$ and R_t, R_0, ε are real-time resistance, original state resistance, and mechanical strain (%) of IKG-I_4, respectively (Wang et al. 2022a, b, c). Regarding the use of IKG-I_4 to install a strain sensor, its strain sensitivity was studied in Fig. 5e. As seen, the GF of IKG-I_4 was 3.25 in the range of 0 to 500%. The responding time of the sensor was only 100 ms in the stretching process, and in the recovery process, the recovery time was 513 ms, which met the requirements of a strain sensor (in Fig. 5f). As depicted in Fig. 5g, the ionogel sensors exhibited extraordinary properties of conductivity, tensile strength, transmittance, response time, and elongation at break compared with ionogel sensors reported in the literature (Tie et al. 2022; Sun et al. 2019; Kim et al. 2023; Huang et al. 2023; Klepić et al. 2020; Song et al. 2022; Wu et al. 2022a, b; Xu et al. 2021). Therefore, as a promising and flexible biomass-based functional material, IKG-I_4 ionogel could meet the high sensitivity and durability requirements of sensors to detect human motion.

Human body movement detection

With the application of the PARSTAT MC electrochemical workstation, the signal produced by the tensile strain of the ionogels can be transmitted to the Bluetooth device in a mobile phone. The movement was first transformed into signals after immobilizing the sensor on different parts of the human body. As shown in Fig. 6, different movements represented diverse curves, and the current increased when the movement range increased. Moreover, different angles of 30, 60, and 90° that the finger bent were also detected by sensors fixed on the finger joints in real-time, and the current gradually decreased simultaneously. Therefore, the change in the current could accurately reflect the bending angles of fingers. Other movements were also tested, such as nodding, jumping, walking, elbow bending, and wrist bending. The sensor showed excellent sensitivity during the cycles without any apparent current loss. In short, the IKG-I_x is competent to be an ideal sensor for real-time monitoring and body movement detection with longevity and stability.

Conclusion

In this work, the KGM biomass polymer was introduced in the ionic solution, and a novel conductive ionogel was synthesized for the first time. By adding new substrates, the resulting ionogels exhibited excellent tensile strength (the highest and lowest detection limits were 2.77 MPa,

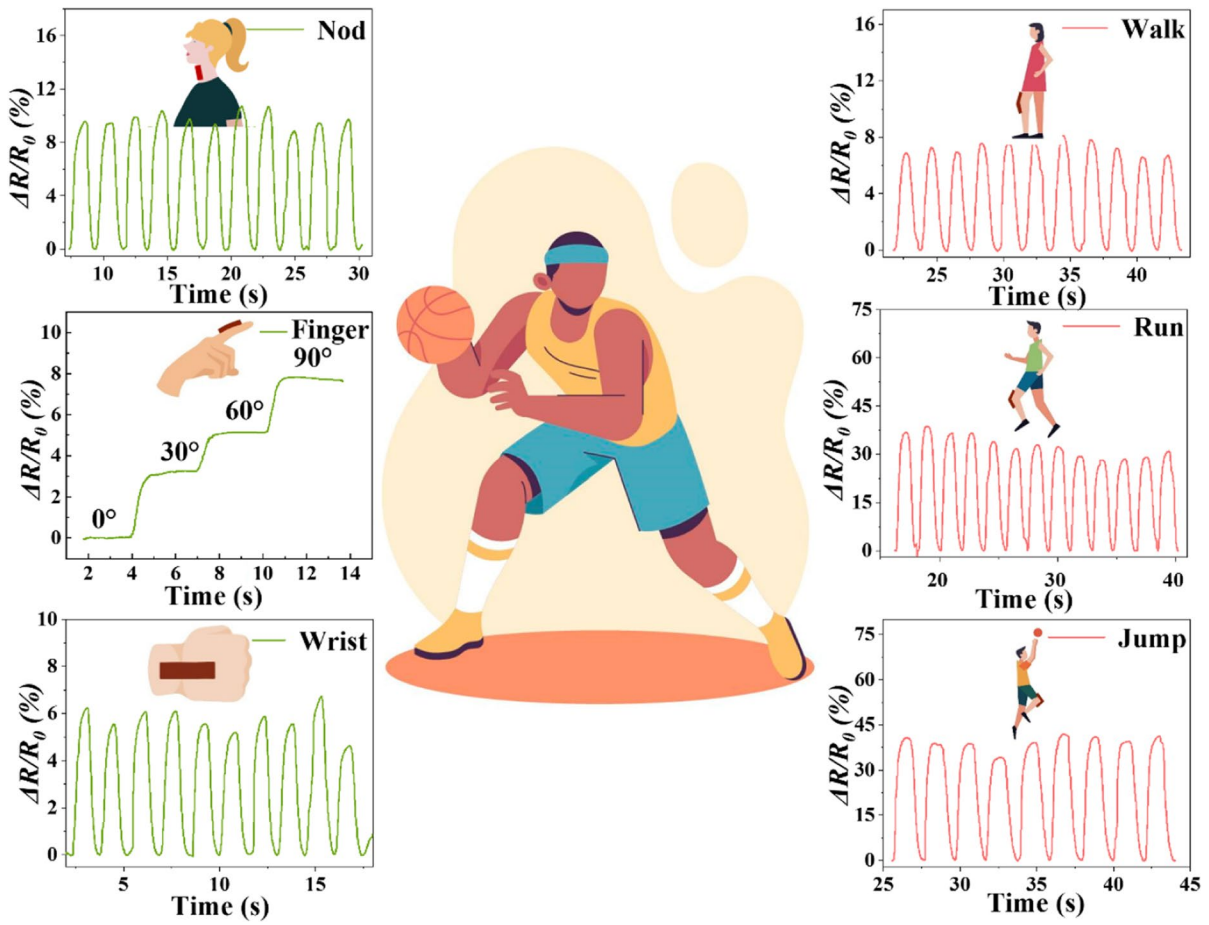

Fig. 6 Variation of electrical signals detecting different human body movements. (Nodding, finger bending, wrist bending, walking, running, and jumping)

997%, and 2.76 MPa, 955%, respectively), durability (1000 cycles), optical transparency (84%, 2 mm), high conductivity (3.94 mS/cm), and environmental tolerance. The ionogel was used as a flexible sensor to detect human movements, including neck bending, elbow bending, knee bending, or subtle movements such as finger bending. Moreover, as a biomass subsistence, KGM is environmentally friendly and easily available, which decreases the cost of synthesizing flexible sensors with high mechanical properties. Based on the superior properties, assembling the ionogels as flexible sensors successfully monitored different ranges of human body movements with high stability and accuracy.

Acknowledgements I would like to express my gratitude to the College of Biomass Science and Engineering, Sichuan University, my supervisor and my senior apprentices in the research group.

Author contributions Zhifan Ye: Conceptualization, Methodology, Visualization, Investigation, Writing-original draft. Min Yang: Modification. Yijia Zheng: Visualization, Methodology, Data curation. Qihan Jia: Validation, Investigation. Haibo Wang: Resources. Junjie Xiong: Investigation. Shuang Wang: Investigation, Visualization, Methodology.

Funding This work was funded by Support Plan of Science and Technology Department of Sichuan Province, China (NO. 2022YFG0273, 2023YFS0168, 2023NSFSC0308, 2023YFS0460), Sichuan University "0 to one" innovation research project (NO. 2022SCUH0024), Sichuan University Postdoctoral Interdisciplinary Innovation Fund (NO. JCXK2229), Fundamental Research Funds for the Central Universities (NO. 2023SCU12107). The authors would appreciate Hui Wang from Pub-Lab Platform, West China School of Basic Medical Sciences and Forensic Medicine, Sichuan University for assistance with the testing process.

Data availability The Data used in this study are available from corresponding authors on reasonable request.

Declarations

Consent for publication All authors revised the manuscript and agreed with the publication.

Competing interests The authors declare no competing interests.

References

Ahmed S, Bui MPN, Abbas A (2016) Paper-based chemical and biological sensors: engineering aspects. Biosens Bioelectron 77:249–263. https://doi.org/10.1016/j.bios.2015.09.038

Cao Y, Huang G, Li X, Guo L, Xiao J (2022) Complex coacervation of carboxymethyl konjac glucomannan and ovalbumin and coacervate characterization. J Dispersion Sci Technol 43:1991–2001. https://doi.org/10.1080/01932691.2021.1888747

Chen L, Chang X, Chen J, Zhu Y (2022) Ultrastretchable, antifreezing, and high-performance strain sensor based on a muscle-inspired anisotropic conductive hydrogel for human motion monitoring and wireless transmission. Appl Mater Interfaces 14:43833–43843. https://doi.org/10.1021/acsami.2c14120

Chen Z, Chen Y, Hedenqvist MS, Chen C, Cai C, Li H, Liu H, Fu J (2021) Multifunctional conductive hydrogels and their applications as smart wearable devices. J Mater Chem B 9:2561–2583. https://doi.org/10.1039/d0tb02929g

Gao Y, Hu Y, Wang J, Ahmad H, Zhu J (2023) Modification of low-salt myofibrillar protein using combined ultrasound pre-treatment and konjac glucomannan for improving gelling properties: intermolecular interaction and filling effect. Int J Biol Macromol 250:126195. https://doi.org/10.1016/j.ijbiomac.2023.126195

Gao Y, Zhang Y, Feng C, Chu H, Feng C, Wang H, Wu L, Yin S, Liu C, Chen H, Li Z, Zou Z, Tang L (2022) A chromosome-level genome assembly of Amorphophallus konjac provides insights into konjac glucomannan biosynthesis. Comput Struct Biotechnol J 20:1002–1011. https://doi.org/10.1016/j.csbj.2022.02.009

Hajiali F, Jin T, Yang G, Santos M, Lam E, Moores A (2022) Mechanochemical transformations of biomass into functional materials. Chem Sustain Energy Mater 15:e202102535. https://doi.org/10.1002/cssc.202102535

Hou C, Xu Z, Qiu W, Wu R, Wang Y, Xu Q, Liu X, Guo W (2019) A biodegradable and stretchable protein-based sensor as artificial electronic skin for human motion detection. Small 15:1805084. https://doi.org/10.1002/smll.201805084

Hu Y, Tian J, Zou J, Zou J, Yuan X, Li J, Liang H, Zhan F, Li B (2019) Partial removal of acetyl groups in konjac glucomannan significantly improved the rheological properties and texture of konjac glucomannan and κ-carrageenan blends. Int J Biol Macromol 123:1165–1171. https://doi.org/10.1016/j.ijbiomac.2018.10.190

Huang Y, Zhao X, Ke J, Zha X, Yang J, Yang W (2023) Engineering nanoscale solid networks of ionogel for enhanced thermoelectric power output and excellent mechanical properties. Chem Eng J 456:141156. https://doi.org/10.1016/j.cej.2022.141156

Jiang N, Chang X, Hu D, Chen L, Wang Y, Chen J, Zhu Y (2021) Flexible, transparent, and antibacterial ionogels toward highly sensitive strain and temperature sensors. Chem Eng J 424:130418. https://doi.org/10.1016/j.cej.2021.130418

Kabanda MM, Bahadur I (2023) Preferred intermolecular cation···anion interactions within the [EMIM][DCA] ionic liquid and its interaction with a water co-solvent molecule. J Mol Liq 381:121804. https://doi.org/10.1016/j.molliq.2023.121804

Kalambate PK, Rao Z, Dhanjai WuJ, Shen Y, Boddula R, Huang Y (2020) Electrochemical (bio) sensors go green.

Biosens Bioelectron 163:112270. https://doi.org/10.1016/j.bios.2020.112270

Kim J, Choi H, Rye H, Yoon K, Lee D (2020) A Study on the red clay binder stabilized with a polymer aqueous solution. Polymers 13:54. https://doi.org/10.3390/polym13010054

Kim J, Kim J-W, Keum K, Lee H, Jung G, Mihyeon P, Lee Y, Kim S, Ha J (2023) A multi-responsive self-healing and air-stable ionogel for a vertically integrated device comprised of flexible supercapacitor and strain sensor. Chem Eng J 457:141278. https://doi.org/10.1016/j.cej.2023.141278

Klepić M, Setničková K, Lanč M, Zák M, Izák P, Dendisová M, Fuoco A, Jansen JC, Friess K (2020) Permeation and sorption properties of CO2 -selective blend membranes based on polyvinyl alcohol (PVA) and 1-ethyl-3-methylimidazolium dicyanamide ([EMIM][DCA]) ionic liquid for effective CO2 /H2 separation. J Membr Sci 597:117623. https://doi.org/10.1016/j.memsci.2019.117623

Li W, Fan Q, Chai C, Chu Y, Hao J (2023) Ti3C2-MXene ionogel with long-term stability and high sensitivity for wearable piezoresistive sensors. Colloids Surf, A 665:131202. https://doi.org/10.1016/j.colsurfa.2023.131202

Liao M, Wan P, Wen J, Gong M, Wu X, Wang Y, Shi R, Zhang L (2017) Wearable, healable, and adhesive epidermal sensors assembled from mussel-inspired conductive hybrid hydrogel framework. Adv Func Mater 27:1703852. https://doi.org/10.1002/adfm.201703852

Lipomi DJ, Vosgueritchian M, Tee BCK, Hellstrom SL, Lee JA, Fox CH, Bao Z (2011) Skin-like pressure and strain sensors based on transparent elastic films of carbon nanotubes. Nat Nanotechnol 6:788–792. https://doi.org/10.1038/nnano.2011.184

Pang Y, Zhang K, Yang Z, Jiang S, Ju Z, Li Y, Wang X, Wang D, Jian M, Zhang Y, Liang R, Tian H, Yang Y, Ren T (2018) Epidermis microstructure inspired graphene pressure sensor with random distributed spinosum for high sensitivity and large linearity. ACS Nano 12:2346–2354. https://doi.org/10.1021/acsnano.7b07613

Rezaei FS, Sharifianjazi F, Esmaeilkhanian A, Salehi E (2021) Chitosan films and scaffolds for regenerative medicine applications: a review. Carbohyd Polym 273:118631. https://doi.org/10.1016/j.carbpol.2021.118631

Seabra AB, Bernardes JS, Fávaro WJ, Paula AJ, Durán N (2018) Cellulose nanocrystals as carriers in medicine and their toxicities: a review. Carbohyd Polym 181:514–527. https://doi.org/10.1016/j.carbpol.2017.12.014

Song H, Yu X, Nguyen D, Zhang C, Liu T (2022) Highly stretchable, self-healable and self-adhesive polyzwitterion ionogels enabled with binary noncovalent interactions. Compos Commun 34:101251. https://doi.org/10.1016/j.coco.2022.101251

Strauss K, Chmielewski J (2016) Advances in the design and higher-order assembly of collagen mimetic peptides for regenerative medicine. Curr Opin Biotechnol 46:34–41. https://doi.org/10.1016/j.copbio.2016.10.013

Sun L, Chen S, Guo Y, Song J, Zhang L, Xiao L, Guan Q, You Z (2019) Ionogel-based, highly stretchable, transparent, durable triboelectric nanogenerators for energy harvesting and motion sensing over a wide temperature range. Nano Energy 63:103847. https://doi.org/10.1016/j.nanoen.2019.06.043

Sun Y, Wang S, Du X, Du Z, Wang H, Cheng X (2021) Skin-conformal MXene-doped wearable sensors with self-adhesive, dual-mode sensing, and high sensitivity for human motions and wireless monitoring. J Mater Chem B 9:8667–8675. https://doi.org/10.1039/d1tb01769a

Tie F, Mao Z, Zhang L, Zhong Y, Sui X, Xu H (2022) Conductive ionogel with underwater adhesion and stability as multimodal sensor for contactless signal propagation and wearable devices. Compos B Eng 232:109612. https://doi.org/10.1016/j.compositesb.2022.109612

Wang H, Li X, Ji Y, Xu J, Ye Z, Wang S, Du X (2022a) Highly transparent, mechanical, and self-adhesive zwitterionic conductive hydrogels with polyurethane as a cross-linker for wireless strain sensors. J Mater Chem B 10:2933–2943. https://doi.org/10.1039/d2tb00157h

Wang H, Xiang J, Wen X, Du X, Wang Y, Du Z, Cheng X, Wang S (2022b) Multifunctional skin-inspired resilient MXene-embedded nanocomposite hydrogels for wireless wearable electronics. Compos A Appl Sci Manuf 155:106835. https://doi.org/10.1016/j.compositesa.2022.106835

Wang H, Xu J, Li K, Dong Y, Du Z, Wang S (2022c) Highly stretchable, self-healable, and self-adhesive ionogels with efficient antibacterial performances for a highly sensitive wearable strain sensor. J Mater Chem B 10:1301–1307. https://doi.org/10.1039/d2tb00041e

Wang S, Xiang J, Sun Y, Wang H, Du X, Cheng X, Du Z, Wang H (2021) Skin-inspired nanofibrillated cellulose-reinforced hydrogels with high mechanical strength, long-term antibacterial, and self-recovery ability for wearable strain/pressure sensors. Carbohyd Polym 261:117894. https://doi.org/10.1016/j.carbpol.2021.117894

Wu D, Yu S, Liang H, He C, Li J, Li B (2020) The influence of deacetylation degree of konjac glucomannan on rheological and gel properties of konjac glucomannan/κ-carrageenan mixed system. Food Hydrocoll 101:105523. https://doi.org/10.1016/j.foodhyd.2019.105523

Wu H, Wu H, Qing Y, Wu C, Pang J (2022a) KGM/chitosan bio-nanocomposite films reinforced with ZNPs: colloidal, physical, mechanical and structural attributes. Food Packag Shelf Life 33:100870. https://doi.org/10.1016/j.fpsl.2022.100870

Wu Y, Ren Y, Liang Y, Li Y (2022b) Semi-IPN ionogel based on poly (ionic liquids)/xanthan gum for highly sensitive pressure sensor. Int J Biol Macromol 223:327–334. https://doi.org/10.1016/j.ijbiomac.2022.10.263

Xiang S, He X, Zheng F, Lu Q (2022) Multifunctional flexible sensors based on ionogel composed entirely of ionic liquid with long alkyl chains for enhancing mechanical properties. Chem Eng J 439:135644. https://doi.org/10.1016/j.cej.2022.135644

Xie F, Gao X, Yu Y, Lu F, Zheng L (2021) Dually cross-linked single network poly(ionic liquid)/ionic liquid ionogels for a flexible strain-humidity bimodal sensor. Soft Matter 17:10918–10925. https://doi.org/10.1039/d1sm01453f

Xu J, Wang H, Du X, Cheng X, Du Z, Wang H (2021) Self-healing, anti-freezing and highly stretchable polyurethane

ionogel as ionic skin for wireless strain sensing. Chem Eng J 426:130724. https://doi.org/10.1016/j.cej.2021.130724

Xu J, Wang H, Wen X, Wang S, Wang H (2022) Mechanically strong, wet adhesive, and self-healing polyurethane ionogel enhanced with a semi-interpenetrating network for underwater motion detection. ACS Appl Mater Interfaces 14:54203–54214. https://doi.org/10.1021/acsami.2c15058

Xue R, Zhou N, Yin S, Qian Z, Dai Z, Xiong Y (2023) All-polymer dynamical ionogel-like materials with benzyl-mediated ultra-strong adhesion for flexible sensor application. Chem Eng J 465:143072. https://doi.org/10.1016/j.cej.2023.143072

Zhang K, Ge F, Tang F, Tan L, Qiu Y, Zhu X (2023) A structure-property study for konjac glucomannan and guar galactomannan: Selective carboxylation and scale inhibition. Carbohyd Polym 299:120220. https://doi.org/10.1016/j.carbpol.2022.120220

Zhou J, Zhuo F, Long X, Liu Y, Lu H, Lou J, Chen L, Dong S, Fu Y, Duang H (2022) Bio-inspired, super-stretchable and self-adhesive hybrid hydrogel with SC-PDA/GO-Ca2+/PAM framework for high precision wearable sensors. Chem Eng J 447:137259. https://doi.org/10.1016/j.cej.2022.137259

Zhou Q, Wang Y, Zhu T, Lian M, Nguyen D, Zhang C (2023) Highly stretchable, self-healable and wide temperature-tolerant deep eutectic solvent-based composite ionogels for skin-inspired strain sensors. Compos Commun 41:101658. https://doi.org/10.1016/j.coco.2023.101658

Zhu A, Huang J, Xie H, Yue W, Qin S, Zhang F, Xu Q (2022) Use of a superbase/DMSO/CO2 solvent in order to incorporate cellulose into organic ionogel electrolyte for flexible supercapacitors. Chem Eng J 446:137032. https://doi.org/10.1016/j.cej.2022.137032

Zhu F (2018) Modifications of konjac glucomannan for diverse applications. Food Chem 256:419–426. https://doi.org/10.1016/j.foodchem.2018.02.151

Zhu M, Jin H, Shao T, Li Y, Liu J, Gan L, Long M (2020) Polysaccharide-based fast self-healing ion gel based on acylhydrazone and metal coordination bonds. Mater Des 192:108723. https://doi.org/10.1016/j.matdes.2020.108723